LASER PENETRATION IN A POWDER BED DURING SELECTIVE LASER SINTERING OF METAL POWDERS: SIMULATIONS VERSUS EXPERIMENTS

T. Laoui[1], X. Wang[2], T. H. C. Childs[3], J. P. Kruth[2], L. Froyen[1]

[1]Dept. of Metallurgy & Materials Engineering, University of Leuven, Heverlee, Belgium
[2]Dept. of Mechanical Engineering, University of Leuven (KULeuven), Heverlee, Belgium
[3]School of Mechanical Engineering, University of Leeds, LS2 9JT, UK

Abstract

To gain a better understanding and control of the Selective Laser Sintering (SLS) process, more fundamental and modeling work is needed. A simple analytical ray-tracing model has been developed to simulate the energy absorption and penetration in SLS. The model is applied to Fe-Cu and WC-Co powder mixtures, irradiated by Nd-YAG or CO_2 laser. It gives an evaluation of the total energy incoupling and optical penetration of the laser beam in a powder bed and an estimation of the sintering zone dimensions. Another model, which considers heat flow by conduction in the bed, has also been used to estimate the sintering dimensions of one laser track.

Introduction

Selective Laser Sintering (SLS) is a rapid prototyping process with a great promise for direct sintering of metal powders to produce 3D functional parts. SLS is utilized to produce parts from polymer powders, polymer coated foundry sand or metal particles, and from relatively low melting point metal powders (e.g. bronze) [1-2]. The consolidation mechanism used in those cases is either through melting of the particles or melting of an easy melting binder (mostly polymer). In order to contribute to the advancement of the SLS process and reduce the production costs, direct laser sintering was applied to commercially available metal powders instead of using proprietary powders. Liquid Phase Sintering (LPS) was used successfully as a consolidation mechanism to sinter high strength powder mixtures (such as Fe-Cu, WC-Co, TiC-Ni) [3-5].

The present work reports the initial modeling work on the laser penetration into a metal powder bed. A simple analytical ray-tracing model has been developed based on two principles: the powder bed construction (a random assemblage of spherical particles), and ray reflection and penetration. Another model, which takes into account the heat flow by conduction in the bed powder, has also been used to estimate the sintering dimensions of a single laser track. Simulations were realized for Fe-Cu and WC-Co powder systems using Nd-YAG and CO_2 lasers.

Ray-tracing model

An analytical ray-tracing model has been developed for evaluating the total energy incoupling (the ratio between the absorbed and the total input energy) and optical penetration of the laser beam (energy absorption profile in the powder bed depth), and for estimating the sintering zone dimensions (thickness/depth and width of a sintered laser track). Further details of the model can be found elsewhere [6]. The model is based on the following assumptions:

- A mixture of two powders is used. The particles are perfect spheres.
- The particles of the two materials are randomly distributed in space;
- The laser beam strikes the powders perpendicularly to the powder bed surface;
- The particles have a specular reflectivity;
- The absorption coefficients are independent of the incident angle and of the temperature;
- The powder bed is put in vacuum

These assumptions are indispensable but can be modified or extended. All rays originate from the plane z = 0 and strike the powder bed surface vertically. At each impingement on a particle, a part of the energy of an emitted ray is absorbed and the rest is reflected. This reflection is assumed to follow a specular reflection law. No energy is lost in the pores between the particles. An emitted ray will be considered to disappear either when it is reflected outside the powder bed or when its energy becomes negligible after several hits against particles.

Results and validation

The experimental data are obtained by laser sintering (with Nd-YAG and CO_2 lasers) of a mixture of two metal powders: the structural powder (Fe, WC) and the binder (Cu, Co) [7]. In the model, the diameters of the powder particles used are 50 µm (Fe), 30 µm (Cu), 50 µm (WC) and 20 µm (Co). The powder assemblage is constructed for the Fe-30wt%Cu powder mixture with 7623 spheres: 2779 Fe spheres and 4844 Cu spheres. The porosity in the powder bed model is about 0.75. For the WC-9wt%Co powder mixture, a total number of 13135 spheres (3488 WC and 9647 Co spheres) was used with a porosity of about 0.73.

Experimental validation

The total energy incoupling as a function of the absorption coefficient of the individual particles is used to validate the present model. The comparison to measurements is shown in Fig. 1, together with the curves obtained by another model developed by B. Van der Scheuren [8]. A good agreement is found between experimental measurements reported for pure elements in literature [9,10] and present simulations.

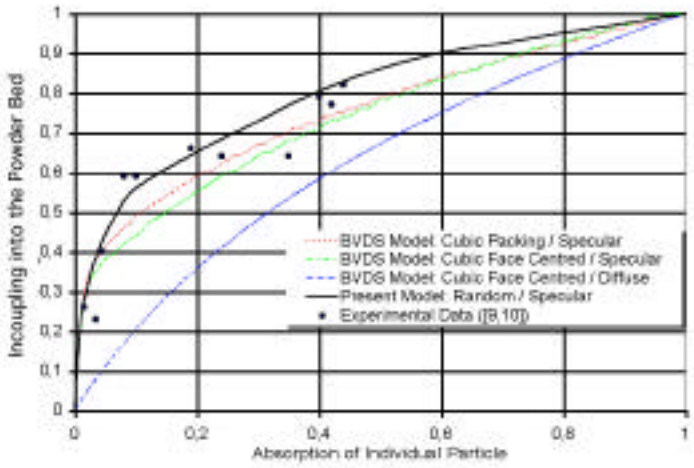

Fig. 1 : Experimental validation of the model

Energy absorption

The absorption coefficients of the pure materials used in this study are shown in Table 1. Some of the values reported in Table 1 were obtained from experimental measurements reported in literature (Fe, Cu), while other values were either calculated from the optical constants (Co) or compared to other similar materials (for WC: it was compared to another carbide, TiC) [9-11].

The simulations consist of emitting a series of randomly located rays. For each laser source, five simulations (tests) are realized, which give slightly different results. The incoupling for two laser sources are shown in Table 2.

Table 1 : Absorption coefficients of the solid materials

Materials	**Absorption coefficients**	
	YAG (_=1.06 _m)	CO_2 (_=10.6 _m)
Fe	0.3	0.035
Cu	0.1	0.015
WC	0.55	-
Co	0.31	0.026

Table 2 : Total energy incoupling

Nd:YAG Laser (_=1.06 _m) Fe-Cu powder mixture			
Tests	E_{total} (%)	E_{Fe} (%)	E_{Cu} (%)
1	65.59	53.61	11.98
2	66.16	52.49	13.66
3	65.49	53.84	11.62
4	65.28	53.23	12.05
5	67.20	55.87	11.34
Average	**65.96**	**53.81**	**12.13**
CO_2 Laser (_=10.6 _m) Fe-Cu powder mixture			
Tests	E_{total} (%)	E_{Fe} (%)	E_{Cu} (%)
1	27.99	22.00	5.994
2	25.71	20.31	5.339
3	26.79	20.88	5.910
4	26.89	21.10	5.791
5	24.81	19.45	5.361
Average	**26.44**	**20.75**	**5.691**
Nd:YAG Laser (_=1.06 _m) WC-Co powder mixture			
Tests	E_{total} (%)	E_{WC} (%)	E_{Co} (%)
1	79.96	61.57	18.39
2	76.63	57.38	19.25
3	81.51	62.59	18.91
4	80.16	61.21	18.95
5	81.82	63.42	18.40
Average	**80.02**	**61.23**	**18.78**

Energy penetration

The absorption profile in depth is used to measure the light energy penetration into the powder bed. The comparison of this penetration between the two laser sources is shown in Fig. 2. From this comparison, we find that the Nd-YAG laser is more absorbed at the surface while the CO_2 laser penetrates deeper into the powder bed.

This is more evident if we compare the ratio of the accumulated energy absorbed up to a certain depth versus the total absorbed energy at full depth of 1 mm (Fig. 3). For example, for Fe-Cu powder bed, we observe 97.5% of the absorbed energy is concentrated within a depth of 0.5 mm for Nd-YAG laser, but only 82.4% within this same depth for CO_2 laser. For WC-Co powder bed, most of the absorbed energy is concentrated within a depth of 0.4mm for Nd-YAG laser.

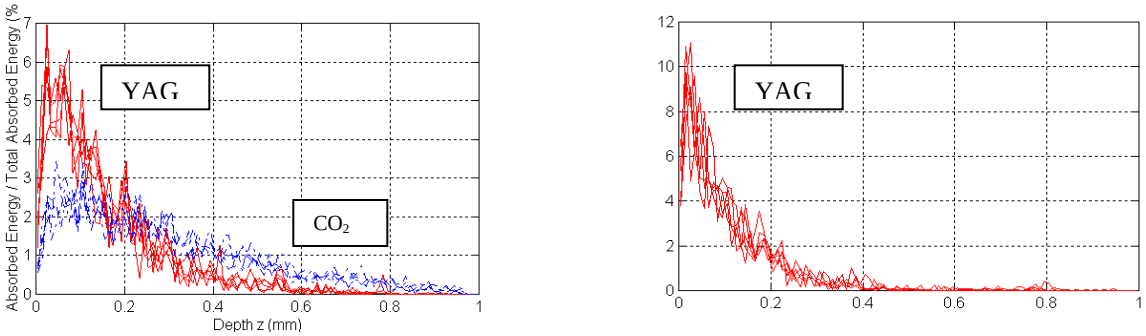

(a) Fe-Cu powder mixture (b) WC-Co powder mixture

Fig. 2 : Absorption profile in depth: comparison of the two lasers

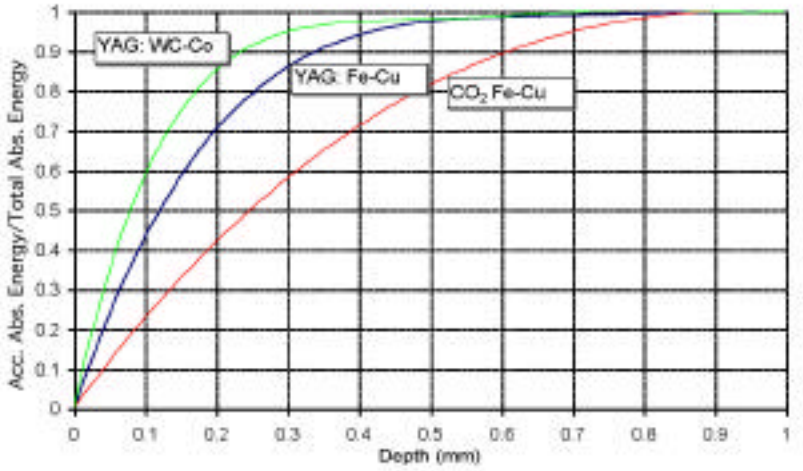

Fig. 3 : Accumulated absorbed energy for both powder systems

This indicates that the energy provided by the Nd-YAG laser is better absorbed by metal powders and thus can be used more efficiently to fuse the powder mixture together by melting the binder particles. On the other hand, the CO_2 laser contributes more to heat that is uselessly dissipated into the powder bed. These simulation results agree well with the trend obtained with

experimental data on laser sintering single layers of both powder systems. An experimental comparative study performed on Fe/steel-Cu and WC-Co powder mixtures with both lasers showed that Nd-YAG laser yielded better results in terms of deeper penetration, higher green density and larger processing window [4,7,12].

Laser beam scanning simulation: estimation of the sintering zone dimension

The large porosity (> 50%) exhibited by the powder bed (point contact between particles) makes it possible to neglect approximately the heat conduction between them. The ray-tracing model may be applied to estimate roughly the dimensions (thickness and width) of a sintered laser track. The relationship between the sintering zone dimensions and the processing parameters is important to optimize the process.

In order to represent a single track sintering, the energy distribution in y-direction (perpendicular to the laser beam scanning direction) in the irradiated zone is given by:

$$E_{ray} = \frac{8W\sqrt{d^2 - 4y^2}}{\pi v d^2} \qquad y \leq \frac{1}{2} d \tag{2}$$

where W is the power of the laser beam; d is its spot diameter and v is the scan speed. In the scanning direction x, the energy distribution is uniform.

The energy absorbed by each particle is calculated in the simulation. This energy is compared to the energy necessary to fuse the particle, calculated respectively for the two materials according to the following equation:

$$E_m = (c_p \leftrightarrow \Delta T + c_l) \leftrightarrow \rho \leftrightarrow V \tag{3}$$

where c_p (kJ/kgK) is the specific heat, _T (°K) is the temperature increment to melt, c_l (kJ/kg) is the latent melt energy (kJ), _ (kg/dm^3) the density and V (dm^3) the volume of the sphere. The values of the thermochemical data used in the calculation are obtained from literature [13-16]. The sintering zone is evaluated from most side-wise molten particles.

In Fig. 4, the estimated thickness and width of the sintering zone obtained by sintering Fe-30wt%Cu powder with Nd-YAG laser of 28.87 W at different scan speeds are compared to experimental measurements [17]. A general agreement is found even though simulations give only a rough estimation.

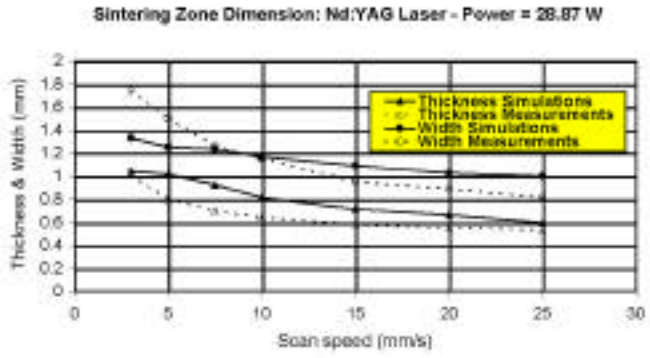

Fig. 4 : Thickness and width versus scan speed for Fe-30%Cu sintered track

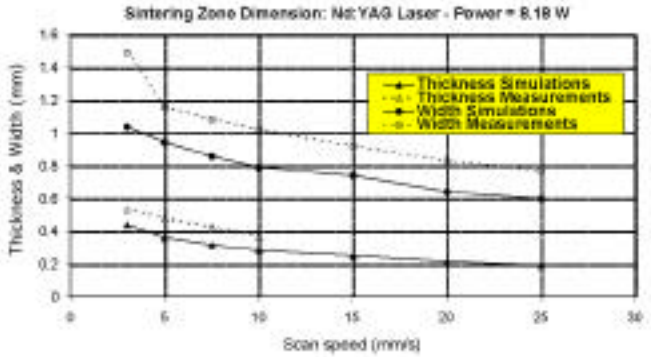

Fig. 5 : Thickness and width versus scan speed for WC-9%Co sintered track

In Fig. 5, the estimated thickness and width of the sintering zone obtained by sintering WC-9wt%Co powder with Nd-YAG laser of ~ 8 W at different scan speeds is compared to experimental measurements [5]. For this powder system, the estimated values of both thickness and width seem to be lower than those measured. One possible reason could be the accuracy of the thermochemical data available for this system (especially for WC). However, the evolution of the sintering zone dimensions (thickness and width) with increasing laser scan speed, for a given laser power, is well described by the model. Nevertheless, more simulations are underway using other processing parameters such as increasing laser power.

Thermally-based model

Tables 3 and 4 also show preliminary simulated results performed on WC-9%Co powder from another model that takes heat flow by conduction in the powder bed into account. The core of this model is a three-dimensional non-linear finite element calculation of the temperature rise caused by the travelling laser beam. It takes into account the influence of both porosity and temperature on the thermal properties (conductivity, specific heat) of the powder bed and the modification to temperature caused by the evolution or absorption of latent heat on melting or solidifying. Density changes in the bed are then estimated from the temperature/time histories of bed elements. In the present case, it has arbitrarily been assumed that a track is created once the melt fraction of the bed's cobalt powder exceeds 0.5. More detail of the modeling is given in [18]. Two sets of simulations are shown. A laser power distribution was assumed uniform (top hat) over the beam diameter of 0.8 mm and absorptivity, following the prior modeling, was supposed to be 0.8. Both simulations are of predicted track width and depth (thickness) for an incident laser power of 8.18W. In one powder bed (Table 3), thermal conductivity at room temperature and the penetration depth of laser radiation into the bed have respectively been assumed to be 0.3 W/mK and 0.25 mm; in the other (Table 4) values of 0.07 W/mK and 0.15 mm have been chosen. It can be seen that the simulations are reasonable at low scan speeds but (unlike the modeling that ignores thermal conduction) differ markedly from experiment at higher speeds. Indeed, no track is predicted to occur at speeds greater than 5 mm/s or 10 mm/s when the powder bed conductivities are taken to be respectively 0.3 W/mK or 0.07 W/mK. The trend in the simulations suggests good agreement with experiment may be obtained by assuming lower conductivity still. For reliable simulation, it is essential that powder conductivity and laser power absorption depth into the bed be established.

Table 3: Simulated and experimental values of thickness and width versus scan speed (Nd-YAG laser, power = 8.18 W) for WC-9%Co sintered track. For simulations, a laser penetration depth of 0.25mm and powder conductivity of 0.3 W/mK were assumed

Scan speed (mm/s)	Sintering thickness (mm)		Sintering width (mm)	
	Simulation	measurement	simulation	measurement
3	0.55	0.53	0.98	1.51
4	0.42	0.51	0.55	1.35
5	0.0	0.48	0.0	1.18

Table 4: Simulated and experimental values of thickness and width versus scan speed (Nd-YAG laser, power = 8.18 W) for WC-9%Co sintered track. For simulations, a laser penetration depth of 0.15mm and powder conductivity of 0.07 W/mK were assumed

Scan speed (mm/s)	Sintering thickness (mm)		Sintering width (mm)	
	Simulation	measurement	simulation	measurement
3	0.55	0.53	1.23	1.51
5	0.40	0.48	0.93	1.18
8	0.25	0.40	0.64	1.07
10	0.0	0.37	0.0	1.03

It is also interesting to compare the assumptions of the two types of models that have led to the simulations reported here. The first model, that ignores thermal conductivity, demonstrates that scattering/reflection of laser power in the surface of the bed, for this low conductivity powder, can approximately set the dimensions of the track; in particular, side-ways scattering can cause the track width to be wider than the laser beam width. In the second model, laser power absorption is assumed to be constrained to the laser beam width, though a depth of penetration is allowed; it shows that conductivity can alternatively explain the trend of track dimensions. Further simulations, currently being carried out, show better agreement with experiments the larger is the absorbed laser power (as might be expected as the track boundaries spread further from the absorption region). Probably a combination of both models will finally yield good agreement with experiment. Both highlight the need for good input data of powder bed characteristics with respect to heat input and flow.

Conclusion

The simulation results show that the developed ray-tracing model gives a good estimation not only of the energy absorption and penetration into the powder bed but also of the sintering zone dimensions (width and thickness) of a sintered laser track. Good agreement has been obtained between measured and predicted dimensions for the Fe-30%Cu tracks. For the WC-9%Co system, the measured values are a bit lower than predicted. Similar results were obtained with a thermally-based model. The trend in the simulations suggests good agreement with experiment may be obtained by choosing good input data of powder bed characteristics. Nevertheless for both models, the rates of change of track dimensions with scan speed are the same for the experiments and simulations

Concerning the two laser sources, it is found that the YAG laser is more efficient in the direct SLS of metal parts: it is absorbed more and the absorbed energy contributes more to the binder melting, while the CO_2 laser contributes more to heat that is uselessly dissipated deeper into the powder bed.

Acknowledgments

This research is supported by the national fund IUAP/PAI P4/33.

References

1. K. McAlea, U. Heymadi, Selective Laser Sintering of metal molds: the RapidTool process. Solid Freeform Fabrication Symposium, pp. 97–104, 1996
2. U. Behrendt, M. Shellabear, The EOS Rapid Prototyping concept. Computers in Industry, 28, pp. 57–61, 1995
3. B. Van der Schueren, J.-P. Kruth, Laser based Selective Metal Powder Sintering: a feasibility study, Proc. 26th CIRP Sem. On Manufacturing Systems LANE'94, pp. 793–802, 1994
4. T. Laoui, L. Froyen, J.-P. Kruth, Selective Laser Sintering of Hard Metal Powders, Proc. Rapid Prototyping and Manufacturing '98 Conf. , pp. 435–467, 1998
5. J.-P. Kruth, L. Froyen, B. Morren, J. Bonse, Selective Laser Sintering of WC-Co "hard metal" parts, Proc. 8th Int. Conf. on Production Engineering, pp. 149–156, 1997
6. T. Laoui, X. Wang, J.P. Kruth, L. Froyen, Modeling of laser penetration in a powder bed during Selective Laser Sintering of metal powders, Proceedings of the 8th European Conference on Rapid Prototyping – 'Research on RP Process', Paris, France, May 3-4, 2000.
7. J.P. Kruth, P. Peeters, T. Smolderen, J. Bonse, T. Laoui, L. Froyen, Comparison of CO_2 and Nd-YAG lasers for use with Selective Laser Sintering of Steel-Copper powders, International Journal of CADCAM and Computer Graphics, vol. 13, No. 4-6, pp. 95-110, 1998
8. B. Van der Scheuren, Basic contribution to the development of the selective metal powder sintering process, Ph.D. Thesis, Faculty of Engineering, K.U. Leuven, 1996
9. N.K. Tolochko, T. Laoui, Y.V. Khlopkov, S.E. Mozzharov, V.I. Titov, M.B. Ignatiev, Absorptance of Powder Materials Suitable for Laser Sintering, Rapid Prototyping Journal vol. 6, No. 3, 2000
10. W.W. Duley, Laser processing and analysis of materials, Plenum press, New York, 1983
11. Handbook of optical constants of solids, Ed. Edward D. Palik, Academic Press inc., New York, 1985 & 1991
12. B. Lauwers, J.P. Kruth, S. Oorts, P. Hespel, J. Bonse, L. Froyen, T. Laoui, Comparison between Nd-YAG and CO_2 lasers for use with Selective Laser Sintering of Metal Powders, Proceedings PHOTOMEC'99, Liège, Belgium, Nov. 25-26, pp. 165-173, 1999
13. I. Barin, Thermochemical data of pure substances, Weinheim, Germany, 1993
14. D.R. Gaskell, Introduction to metallurgical thermodynamics, McGraw-Hill Book Co., 1981
15. H. Ralph et al., Selected values of the thermodynamic properties of binary alloys, ASM, Metals Park, Ohio, 1973
16. Materials Engineering, "Materials Selector", Editors: N. Waterman and M.F. Ashby, Elsevier, Amsterdam, 1992
17. J.-P. Kruth et al, Basic powder metallurgical aspects in selective metal powder sintering, Annals of the CIRP, Vol. 45/1, pp. 183-186, 1996
18. T.H.C. Childs, C. Hauser, C.M. Taylor, A.E. Tontowi, Simulation and experimental studies of crystalline polymer and direct metal selective laser sintering, In this Proceedings, 2000